Superparamagnetic relaxometry (SPMR) for sensitive detection of HER-2 positive tumors in mice

Giulio Paciotti[*], Kayla E. Minser[*], Caroline L. Weldon[*], Andrew Gomez[*], Todor Karaulanov[*], Helen J. Hathaway[**], William H. Anderson[*], Christopher P. Nettles[*], and Dale L. Huber[***], and Erika C. Vreeland[*]

[*]Imagion Biosystems, Inc., Albuquerque, NM, USA, giulio.paciotti@imagionbio.com
[**]University of New Mexico Health Sciences Center and University of New Mexico Comprehensive Cancer Center, Albuquerque, NM, USA, hjhathaway@salud.unm.edu
[***]Center for Integrated Nanotechnologies, Sandia National Laboratories, Albuquerque, NM, USA

ABSTRACT

Superparamagnetic relaxometry (SPMR) is a non-invasive technique that utilizes superconducting quantum interference device (SQUID) detectors to localize and quantify the magnetization of superparamagnetic iron oxide (Fe_3O_4) nanoparticles (NPs) specifically bound to cancerous tumors. In an SPMR measurement, polyethylene glycol (PEG) coated NPs are functionalized with a tumor-targeting monoclonal antibody and injected intravenously. NPs that reach and bind to the target tissue are measured by the MRX™ instrument, while unbound nanoparticles, such as those freely circulating in the bloodstream, are not detected. Here, we demonstrate the use of SPMR for specific detection of HER2 positive tumors in mice using long-circulating anti-HER2 antibody conjugated PrecisionMRX® NPs in vitro and in vivo.

Keywords: HER2, nanoparticles, superparamagnetic, iron oxide, breast cancer

1 INTRODUCTION

Current methods for detecting solid tumors lack sensitivity and diagnose primary and metastatic lesions only after the tumor is well established. Superparamagnetic Relaxometry (SPMR) is a combination technology that utilizes superconducting quantum interference detectors (SQUID) to measure the magnetic relaxation of superparamagnetic tumor-targeting magnetite (Fe_3O_4) nanoparticles [1, 2].

To perform the SPMR measurements, Imagion Biosystems, Inc. carboxylate functionalized PrecisionMRX® nanoparticles [3] are coated with PEG and labeled with a tumor targeting moiety (i.e., a monoclonal antibody (mAb)). These functionalized NPs are intravenously injected to specifically target solid tumors utilizing both passive (i.e., the EPR effect) and active (i.e., receptor mediated) mechanisms. Subsequently, the MRX™ instrument pulses the nanoparticles with a low magnetic field and only those particles that are bound to their target site are measured by the SQUID sensors. Unbound nanoparticles are not detected (Fig. 1).

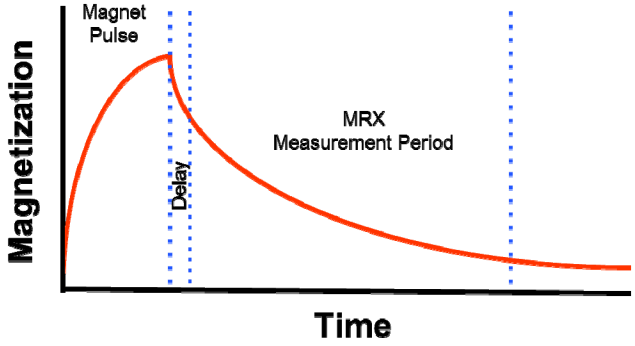

Figure 1. The MRX measurement. At t = 0, a small magnetic field is applied to align the magnetization of the NPs. The magnet is then switched off and following a brief delay, the SPMR measurement begins. The measurement ends after 2.2 seconds. Unbound nanoparticles relax quickly, before the onset of the measurement, and are not detected. Bound nanoaprticles relax relatively slowly, so only NPs bound to cells are detected during the measurement period. (Adapted from [1]).

2 MATERIALS AND METHODS

2.1 Nanoparticle Characterization

To ensure that the PrecisionMRX® Anti-HER2 NPs are suitable for in vitro and in vivo testing several key parameters tested including particle size (to ensure a strong SPMR signal), Anti-HER2 content and potency, and stealth (to ensure extended pharmacokinetics).

PrecisionMRX NP core size was determined by small angle X-ray scattering (SAXS) and transmission electron

microscopy (TEM). Dynamic light scattering (DLS) was used to determine the hydrodynamic diameter and zeta potential of carboxylate (COO^-), PEGylated, or anti-HER2 conjugated PEG NPs.

Functionality of the Anti-HER2 NPs was confirmed by ELISA in which native Anti-HER2 was biotinylated and used as a competitive ligand. Increasing amounts of unbiotinylated Anti-HER2 or Anti-HER2 NPs were added to ELISA wells coated with the extracellular domain of the HER2 antigen. Additionally, every well was pulsed with a fixed mass of the biotinylated Anti-HER2. After a 1 hour incubation, the plates were washed and the biotinylated antibody was detected with alkaline phosphatase labeled streptavidin**.**

The above procedure was adapted to demonstrate the specific binding of the Anti-HER2 NPs to a HER2 overexpressing cell line, MCF7/HER2-18. These cells were generated by stably transfecting the HER2 gene into the low expressing parental cell line, MCF7. For these studies, MCF7/HER2-18 cells were cultured to 80% confluency in T-25 tissue culture flasks. On the day of the experiment, one set of flasks were pulsed with 200 µg of native Anti-HER2 (competitive binding group) and incubated for 2 hours at room temperature. The non-competed flasks were pulsed with PBS. Both sets of flasks were pulsed with 0.5 µg of the anti-HER2 NPs and incubated for an additional hour at room temperature. Subsequently, the media was removed, the cells washed with PBS and harvested using non-enzymatic methods and pelleted by centrifugation. To correlate the SPMR signal with the level of HER2 expression, the above study was repeated using the parental MCF7 cell line. Specific binding was determined by magnetic dipole measurements on the MRX™ instrument and confirmed with digital photography.

For in vivo studies, nude mice with xenograft BT474 or MCF7 tumors were intravenously injected anti-HER2 conjugated PEG NPs at a dose of 20 mg/kg of body mass, while control mice were dosed with 100 µL of saline. Mice were measured individually on the MRX™ instrument after 24 hours and a magnetic dipole map was generated for signal localization. Mice were euthanized and tumor and organs harvested for ex-vivo SPMR measurements.

3 RESULTS

3.1 Nanoparticle Characterization and Functionality

25 nm cores (σ = 1.5 nm) were used for all experiments (Fig. 2). DLS measurements (Table 1) confirm the increasing hydrodynamic diameter of NPs corresponding to PEG coating and the covalent conjugation of the anti-HER2 mAb. The resulting zeta potentials are indicative of the stealth of the NPs in biological environments, with neutrally charged NPs expected to be recognized and removed from circulation by the macrophagocytotic system (MPS) less rapidly than more negatively charged NPs.

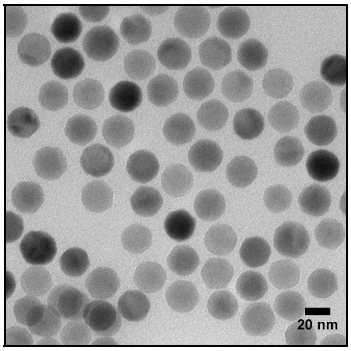

Figure 2. PrecisionMRX® nanoparticle cores.

Surface	Diameter (nm)	PdI	Zeta Potential (mV)
COO^-	46	0.04	-40
PEG	70	0.10	-10
PEG + anti-HER2	85	0.10	0

Table 1. Hydrodynamic diameter and zeta potential of COO^-, PEGylated, or anti-HER2 conjugated PEG NPs.

The competitive ELISA data shown in Fig. 3 support that both the native and anti-HER2 NPs effectively competed out the biotinylated anti-HER2 for the targeted antigen coated on the ELISA wells.

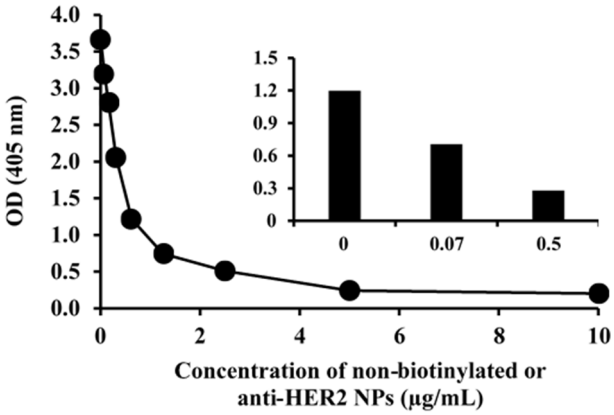

Figure 3. Competition curves for native anti-HER2 Ab and Anti-HER2 conjugated NPs (inset). The graphs show that increasing concentrations of anti-HER2 NPs are able to compete with binding of biotinylated Anti-HER2 with equivalent potency to native anti-HER2 mAb.

3.2 Specific binding of anti-HER2 NPs in vitro

Specific binding of the anti-HER2 NPs to the MCF7/HER2-18 cells is presented in Fig. 4. In Fig. 4A, the non-competed samples generated significant magnetic dipoles, whereas those samples pre-incubated with native anti-HER2 did not. In Fig. 4B, non-competed binding of the anti-HER2 NPs is confirmed by the brown coloration of the cell pellet. The lack of the particles associated with the cell pellet in the competed sample confirms competitive binding of the native anti-HER2 Ab.

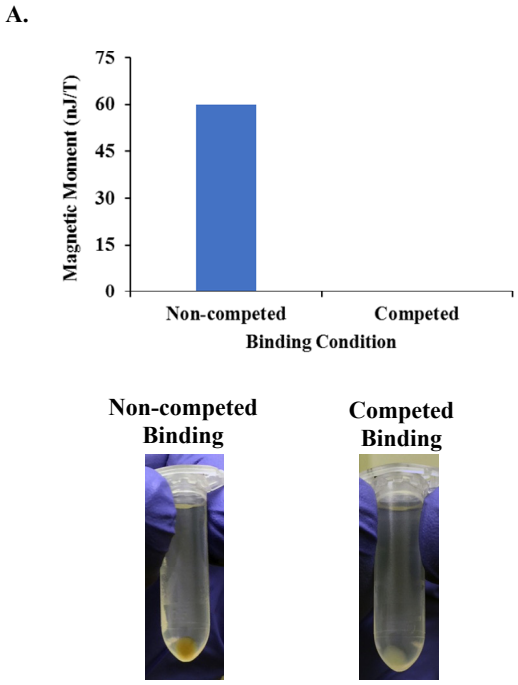

Figure 4. Competitive binding of anti-HER2 conjugated NPs to MCF7/HER2-18 cells as measured by A. the MRX™ instrument and confirmed by B. digital photography.

Fig. 5A further demonstrates that binding of Anti-HER2 NPs corresponds to the expression of the HER2 antigen on the cell surface. FACS analyses of the MCF-7 cells confirmed a minimal level of the HER2 antigen with reposect to the HER2 overexpression measured in the MCF7/HER2-18 variant (data not shown). The digital photograph in Fig. 5B visually confirms a low level of competitive binding in parental MCF7 cells with respect to the transfected MCF7/Her2-18 cells.

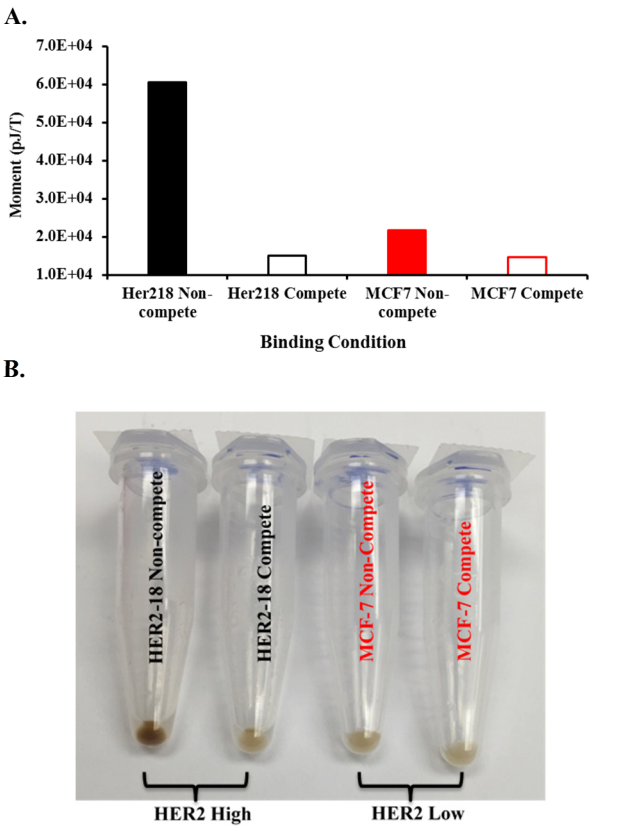

Figure 5. Competitive binding of anti-HER2 conjugated NPs can be correlated to the expression of HER2 on cells. A. MRX™ measurements of MCF7/HER2-18 and parental MCF7 cells confirmed by B. digital photography.

3.3 SPMR detection of HER2 positive tumors in vivo

As shown in Fig. 6, magnetic dipoles were detected in two distinct locations: one at the target site (the tumor), the other at the site of NP elimination (the liver). No measurable signal was detected in control mice.

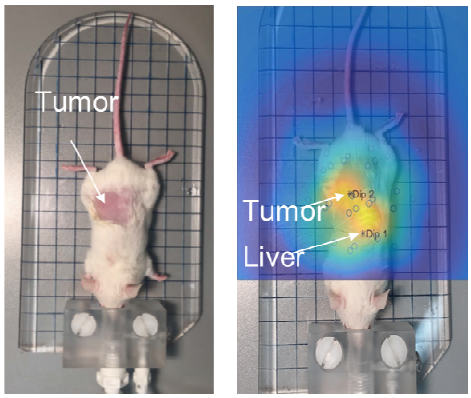

Figure 6. Generated magnetic dipole map following the intravenous injection of anti-HER2 NPs in BT474-tumored mice.

The Anti-HER2 NPs generated a significantly higher dipole moments in the high HER2 expressing BT474 tumors when compared to the low HER2 expressing MCF7 tumors (Fig. 7). This was consistent was both the in vitro studies reported in Figs. 4 and 5 as well as FACS analysis (data not shown). No measurable signal was detected in control mice.

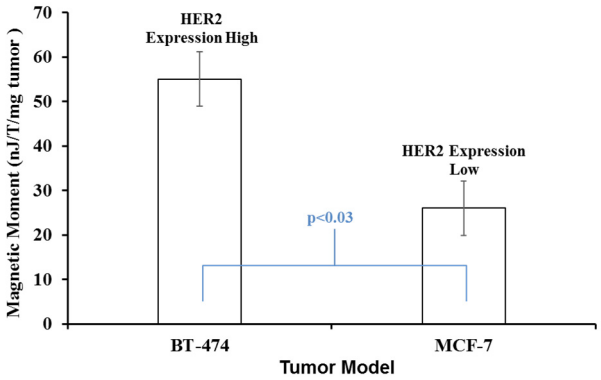

Figure 7. The strength of the magnetic dipole generated by the MagSense-Anti-HER2 particles is dependent on the level of HER2 expression on the cell surface.

4 DISCUSSION AND CONCLUSIONS

In vitro, the Anti-HER2 conjugated MagSense nanoparticles exhibited significant and specific binding to HER2 overexpressing breast cancer cells. Specific binding was defined by the ability of the native mAb to competitively block the binding of the Anti-HER2 NPs to the target antigen. In addition, in low HER2 expressing MCF7 cell lines, the Anti-HER2 NPs exhibited little to no binding.

In vivo, distinct magnetic dipoles were mapped to the target site (i.e., the tumor) and site of nanoparticle elimination (i.e., the liver). Consistent with the in vitro data described above, the Anti-HER2 particles generated significantly higher in vivo dipoles in targeting high HER2 expressing BT-474 tumors in contrast to low-expressing MCF7 tumors.

5 ACKNOWLEDGEMENTS

This work was performed, in part, at the Center for Integrated Nanotechnologies, an Office of Science User Facility operated for the U.S. Department of Energy (DOE) Office of Science. Sandia National Laboratories is a multi-program laboratory managed and operated by Sandia Corporation, a wholly owned subsidiary of Lockheed Martin Corporation, for the U.S. Department of Energy's National Nuclear Security Administration under contract DE-AC04-94AL85000.

REFERENCES

1. De Haro, L.P., et al., *Magnetic relaxometry as applied to sensitive cancer detection and localization.* Biomedical Engineering/Biomedizinische Technik, 2015.
2. Hathaway, H.J., et al., *Detection of breast cancer cells using targeted magnetic nanoparticles and ultra-sensitive magnetic field sensors.* Breast Cancer Res, 2011. **13**(5): p. R108.
3. Vreeland, E.C., et al., *Enhanced Nanoparticle Size Control by Extending LaMer's Mechanism.* Chemistry of Materials, 2015. **27**(17): p. 6059-6066.